A triazole Schiff base-based selective and sensitive fluorescent probe for Zn^{2+}: A combined experimental and theoretical study

Caixia Yuan, Xinyu Liu, Yanbo Wu, Liping Lu *, Miaoli Zhu

Institute of Molecular Science, Key Laboratory of Materials for Energy Conversion and Storage of Shanxi Province,
Key Laboratory of Chemical Biology and Molecular Engineering of the Education Ministry, Shanxi University, Taiyuan, Shanxi 030006, PR China

ABSTRACT

A triazole-Schiff base, 4-(5-Chloro-2-hydroxybenzylideneamino)-1H-1,2,4-triazole-5(4H)-thione (HL), exhibits the high selectivity and sensitivity for Zn^{2+} in the fluorescence spectrometry over other common metal ions, especially Cd^{2+} in DMSO:H$_2$O (1:9, *v/v*) solution. A 1:1 binding ratio of Zn^{2+}/L for the complex has been obtained by Uv–Vis titration experiments and Job's plot with the detection limit of 51 nmol/L. The coordination mode of the complex in solution was further confirmed by density functional theory (DFT) calculations. Time-dependent density functional theory (TD-DFT) calculations indicate that a chelation-enhanced fluorescence (CHEF) effect occurs in the process of detecting Zn ion.

© 2015 Elsevier B.V. All rights reserved.

1. Introduction

Zinc, as an essential life element, is the second most abundant metal ion in the human body after iron [1–2]. It has the potential to perform many important functions in a variety of biological processes including gene transcription, signal transmission and mammalian reproduction [3–5]. Owing to the important role of zinc, several methods for detecting Zn^{2+} in various samples have been developed, such as voltammetry, atomic absorption–emission spectroscopy, inductively coupled plasma-atomic emission spectrometry and fluorescence spectrometry etc. [6–11]. Among these, fluorescence method stands out due to its simplicity, cost effectiveness and high sensitivity [12] and thus had attracted the scientists' interest recently [13–15].

To satisfy the distinct demands, a variety of zinc ion fluorescence sensors have been proposed [16–27]. Recently, the Zn^{2+} sensors based on Schiff base [28–44] and 1,2,4-triazole [12,45–49] developed quickly for their synthetic simplicity, good water-solubility, strong coordination ability (to transition metal ions), and abundant physic-chemical properties. It would be reasonable to believe that the compounds with both Schiff base and 1,2,4-triazole will be the more powerful Zn^{2+} probes. However, to our knowledge, the employment of 1,2,4-triazole-Schiff base as the fluorescence Zn^{2+} probe is not reported so far.

In this work, we reported a simple and effective fluorescent sensor, 4-(5-Chloro-2-hydroxybenzylideneamino)-1H-1,2,4-triazole-5(4H)-thione (HL) (Scheme 1), which exhibits the excellent selectivity and high sensitivity for Zn^{2+} in the fluorescence spectrometry over other essential metal ions, especially Cd^{2+}. The results of the density functional theory (DFT) calculations show that the 1,2,4-triazole and Schiff base parts are not coplanar in the equilibrium structure of the free ground state HL ligand, but they will become coplanar in the equilibrium structure of the excited state of ZnL complex, which will significantly increase the fluorescence intensity, suggesting a chelation-enhanced fluorescence (CHEF)-type sensor. In contrast, they are still not coplanar in the equilibrium structure of the excited state of CdL complex with the very weak fluorescence.

2. Materials and methods

2.1. General

All chemicals were purchased from commercial suppliers without further purification unless specially noted and 4-amino-1H-1,2,4-triazole-5(4H)-thione was prepared as described previously [50]. Double distilled water was used to prepare the solutions of metal ions.

Elemental analyses were performed on VARI-EL elemental analyzer. IR spectra in KBr disks were recorded using Shimadiu-FTIR-8300 Spectrophotometer in the range of 4000–400 cm^{-1}. ^{1}H-NMR spectra were determined with a Bruker 600-NMR spectrometer. The fluorescence and electronic spectra were received with Cary 50 and Cary Eclipse Spectrophotometer (Varian,USA) at room temperature, respectively. DFT calculations were carried out at the B3LYP/6-31G(d) level by using the Gaussian 09 program.

* Corresponding author.
E-mail addresses: luliping@sxu.edu.cn (L. Lu), miaoli@sxu.edu.cn (M. Zhu).
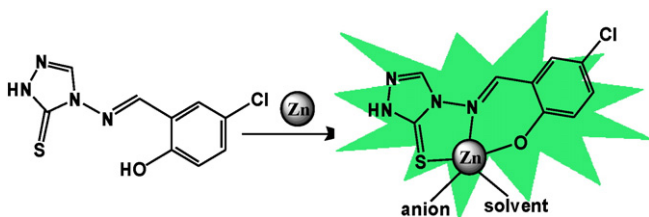
Scheme 1. Structure of the probe HL and proposed binding mode with Zn^{2+}.

2.2. Synthesis of 4-(5-Chloro-2-hydroxybenzylideneamino)-1H-1,2,4-triazole-5(4H)-thione (HL)

The triazole Schiff base was synthesized according to the similar procedure previously reported [51]. A 1.0 mmol (0.115 g) of 4-amino-1H-1,2,4-triazole-5(4H)-thione was thoroughly dissolved in 30 ml of absolute ethanol with a constant stirring at 353 K. Then 1.0 mmol (0.156 g) 5-chlorosalicylaldehyde in 20 ml of absolute ethanol was added dropwise to the above solution. The mixture was refluxed for 2 h. The light yellow precipitates were obtained, filtered out and kept for crystallization dissolving in absolute ethanol. Yield: 68%. Anal. Calcd. for $C_9H_7ClN_4OS$: C 42.44, H 2.77, N 22.00, S 12.59%. Found: C 42.56, H 2.79, N 22.13, S 12.50%. IR (v/cm^{-1}): 1612($v_{C\,=\,N(imine)}$), 1539($v_{C\,=\,N(triazole)}$), 1285(v_{C-O}), 1219($v_{C\,=\,S}$). UV/vis in DMSO, λ_{max}/nm (ε/dm^3 mol^{-1} cm^{-1}): 260(17,600), 342(7620). ^{1}H NMR (DMSO-d_6) 13.98 (1H, NH-triazole), 10.87 (1H, N = CH), 9.75 (1H, OH-Ar), 8.95 (CH-triazole), 7.78–7.02 (3H, CH-Ar).

2.3. General UV–Vis and fluorescence spectra measurements

Stock solutions of the metal ions (0.1 M) were prepared in double distilled water. A stock solution of HL (0.1 M) was prepared in DMSO. The effects on the addition of different metal ions to HL in the DMSO/H$_2$O (1:9, v/v) solution were investigated by UV–Vis and Fluorescence measurements and absorption/fluorescent intensity changes were recorded at the temperature (298 ± 0.5) K after each addition. The limited of detection (LOD) was calculated based on the standard deviation of the response (SD) and the slope of the calibration curve (S) at levels approximating the LOD according to the formula: LOD = 3SD/S.

2.4. Quantum chemical calculations

DFT calculations were performed at the B3LYP/6-31G(d) level to investigate the spectral behaviors of HL and its complexation with Zn^{2+}. The solvation effect was considered for all the calculations by using the polarizable continuum model (PCM). The geometries of the compound and its Zn^{2+} and Cd^{2+} complexes were initially optimized at the ground state potential energy surfaces (PESs). The energies of excited states in this system were calculated with the time-dependent (TD) procedure. The UV–Vis spectra were simulated by the single point TD-DFT calculations at the ground state optimized structures and the fluorescence spectra were calculated by the geometry optimization at excited state potential energy surfaces with the ground state optimized structures as the starting points.

3. Results and discussion

3.1. Binding behavior of HL toward Zn^{2+}

The absorption spectrum of HL exhibits two main bands, respectively, a higher energy band with strong absorption at 267 nm and a low energy broad comparatively weak absorption band at 347 nm. As shown in Fig. 1, with addition of Zn^{2+} (0–2.0 equiv.) to the solution of probe HL (50 μM), the absorption peaks of HL decrease gradually meanwhile two new absorption peaks at 281 nm and 396 nm, respectively, appear
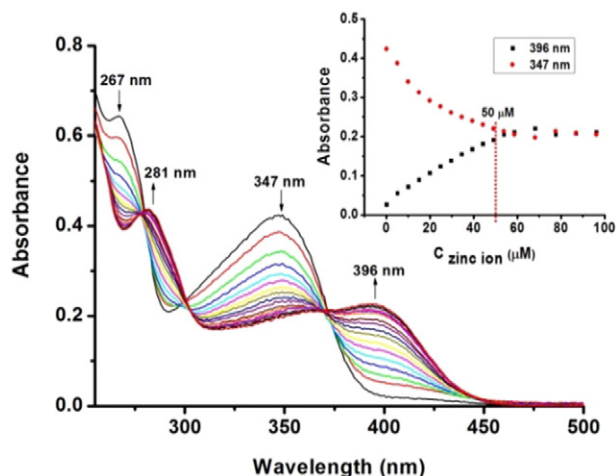

Fig. 1. The changes in UV–Vis absorption spectra of HL(50 μM) upon addition of Zn^{2+}(0–2 equiv.) in DMSO–H$_2$O solution (1:9, V/V). Inset: the absorbance at 347 nm and 396 nm as a function of Zn^{2+} concentration, respectively.

and gradually increase. Correspondingly, there are four isosbestic points at 278, 300, 371, and 451 nm, respectively. The changes in the absorption spectra indicate the formation of a stable complex with a certain stoichiometric ratio between the receptor HL and Zn ion. It's worth noting that the Zn^{2+} concentration of 50 μM is a separation point, from this point on, excrescent Zn^{2+} ions will not lead to the observable change on the absorbance at 281 nm and 396 nm, which implies the formation of new complex with 1:1 binding stoichiometry between HL and Zn^{2+} (Fig. 1, inset). From the spectral titration data (Fig S1A), the determined association constant is 1.96×10^4 M. Moreover, a job's plot depending on absorbance at 396 nm as a function of Zn^{2+} concentration exhibits a maximum point at a mole fraction of 0.5 (Fig. 2), confirming again that the probe HL formed a 1:1 complex with Zn^{2+}.

It is also evident by the proton chemical shift changes that Zn^{2+} binds to HL. From ^{1}H NMR spectrum of the Schiff base HL, the N–H and C–H protons of triazole ring resonate at 13.98 ppm and 8.95 ppm, respectively. A characteristic proton signal at 10.87 ppm and a signal at 9.75 ppm are attributed to –OH and –CH = N, respectively. In addition, the signals for the aromatic ring protons appear in the range of 7.02–7.78 ppm (Fig. S2A). When Zn^{2+} is added, these protons of HL move upfield obviously (Fig. S2B), implying Zn^{2+} coordinating environment enclosed by the amide N, phenolic O and thione S of the ligand. The result is an agreement with the ZnL binding mode advised above.
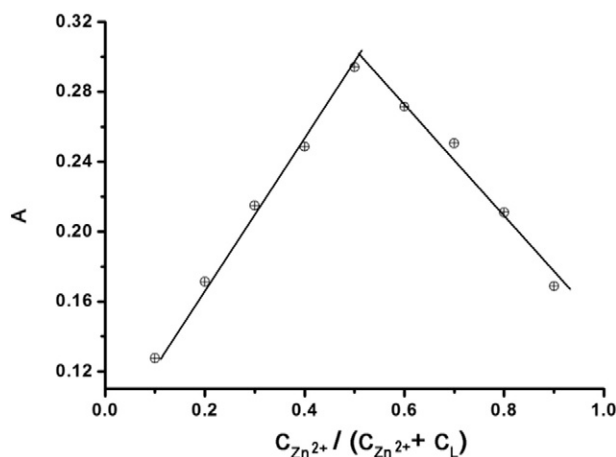

Fig. 2. Job's plot of L–Zn^{2+} complex in DMSO–H$_2$O (1:9) solution. The total molar concentration of HL and Zn^{2+} is 50 μM.

3.2. Fluorescence changes of HL response to Zn^{2+}

A fluorescence titration of Zn^{2+} was conducted using 1 μM solution of the probe HL in DMSO/H_2O (1:9 v/v) system. With the excitation at 396 nm, the probe HL itself has a weak fluorescence emission at about 524 nm (see Fig. 3). When the Zn^{2+} is gradually added to the solution, the emission intensity of the probe HL will increase continuously until 30 equiv. of Zn^{2+} is added to the solution. At this point, the fluorescence intensity to the solution of the probe undergoes a ca. 10-fold increase and the emission maximum shifts from 524 to 504 nm. Meanwhile, a healthy association constant of 1.09×10^4 M is found for the complex (Fig. S1B). Remarkably, a visual fluorescence change (from colorless to green) for HL, upon the addition of Zn^{2+}, was observed under illumination with a UV 365 nm lamp (Fig. 3, inset).

The detection limit of HL for Zn^{2+} was obtained by treating HL (1 μM) with various concentrations of Zn ion (0–0.8 μM) and the emission intensity at 514 nm was plotted as a function of the Zn ion concentration. The emission intensity of probe is linearly proportional to Zn ion concentrations of 0–0.8 μM. Based on the 3σ of the blank as the comparison, the calculated detection limit is 5.1×10^{-8} M, which is lower than most of the reported Zn ion chemosensors based on triazole or Schiff base (Table 1) [19,28–32,45] and therefore indicates a high sensitivity toward the Zn^{2+}. In addition, the fluorescence intensities were obtained for the Zn–L in the different pH value (Fig. S3). When the solution pH is 7.01, the fluorescence emission of Zn–L is the strongest, which is the suitable condition for Zn^{2+} determination.

Reversibility is an important aspect in developing novel chemosensors for practical application. Thus, Na_2EDTA-addition experiment was performed to examine the reversibility of the HL complexation with Zn^{2+} (Fig. S4). As expected, after the addition of EDTA to a mixture of HL and Zn^{2+}, the fluorescence emission intensity is completely quenched, demonstrating that the binding is reversible.

3.3. Selectivity of probe HL for Zn^{2+}

The advantage of using HL compound as the chemosensor of the Zn^{2+} is shown not only by the high sensitivity, but also by the excellent selectivity. In this work, the influence of a variety of metal ions, including Li^+, Na^+, K^+, Mg^{2+}, Ca^{2+}, Ba^{2+}, Al^{3+}, Fe^{3+}, Co^{2+}, Ni^{2+}, Cu^{2+}, Mn^{2+}, Cr^{2+}, Cd^{2+}, Pb^{2+}, Ag^+, to fluorescence properties of the HL solution are measured in DMSO/H_2O (1:9 v/v) system. The fluorescence spectra of solutions of HL (1 μM), recorded within 5 min after the addition 30 equiv. of each of these metal ions, are displayed in Fig. 4 and Fig. S5. From the figures, only the addition of Zn^{2+} promotes
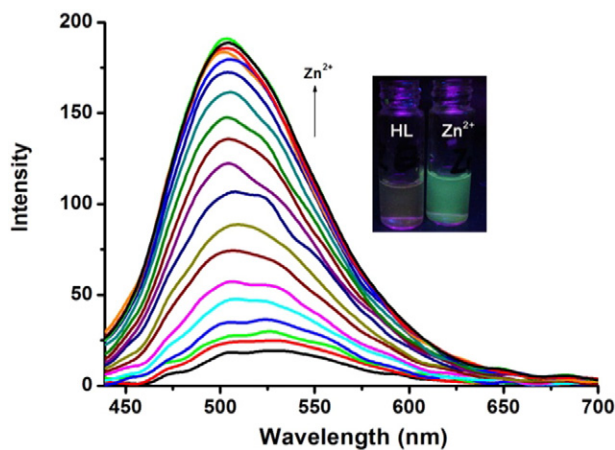
Table 1
A comparison table about the detection limits based on Schiff base or triazole for Zn^{2+}.

Detection limit(M)	Solvent	Signal output	Ref
1.14×10^{-2}	DMF/H_2O(7:3)	Fluorescence	[19]
$1.1 \times 10-6$	HEPES/CH_3OH (99:1)	Absorbance	[28]
1.0×10^{-7}	DMF	Fluorescence	[29]
1×10^{-7}	DMF	Fluorescence	[30]
8.8×10^{-8}	Tris–HCl buffer	Fluorescence	[31]
1.67×10^{-7}	DMF/HEPES(9:1)	Fluorescence	[32]
4.2×10^{-7}	DMSO/H_2O(2:8)	Fluorescence	[45]
5.1×10^{-8}	DMSO/H_2O(1:9)	Fluorescence	This work

the increasement of the fluorescence intensity at 504 nm obviously, while other metal ions do not cause any significant changes of the fluorescence intensity under identical conditions, suggesting the high specificity of HL as the Zn^{2+} sensor. Remarkably again, the color change (nearly colorless to green) associated with the reaction of HL with Zn^{2+} is readily detectable under a lamp at 365 nm because no significant color changes can be observed for the HL solutions with other metal ions. Such color change is useful for the fast visual detection. In addition, the comparative experiments were carried out in the presence of Zn^{2+} mixed with other relevant metal ions. No significant difference in the fluorescence responses of HL for Zn^{2+} was observed by comparing the intensity with the co-existence of other metal ions (Fig. S6).

3.4. DFT calculations

To explain the proposed binding mode and the fluorescence enhancement mechanism, the DFT calculations were carried out for the HL probe, the ZnL complexe, and the CdL complexe at B3LYP/6–31G* level. We constructed several structures for ZnL and CdL complexes with the consideration of 1:1 ratio between HL probe and metal ions, the possible coordination solvent molecules, and possible coordination numbers. The optimized ZnL molecular system forms a nearly tetragonal pyramid structure. The bond lengths between Zn and phenolic oxygen atom or acetate oxygen atom are 2.03489 Å and 1.92340 Å, respectively. Similarly, the Zn–N, and Zn–S bond lengths are 2.06587 and 2.59167 Å, respectively. These data are similar to those in the reported crystal structures of Zn complex with Schiff base ligand [52–54], indicating the reasonability of the complex ZnL with a 1:1 binding mode. The ground state optimized structure of HL as well as the stable structures of ZnL and CdL complexes is shown in Fig. 5. As the figure shows, the 1,2,4-triazole ring and benzene ring of the Schiff base ligand
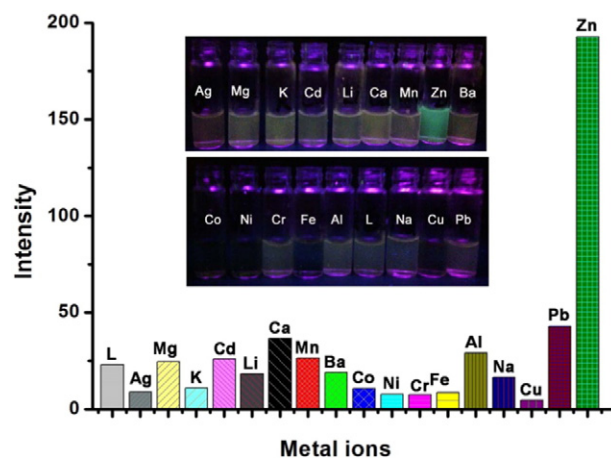

Fig. 3. The fluorescence intensity of HL (1 μM) with various amounts of Zn^{2+} (0–34 equiv.) in DMSO/H_2O solution (1:9 v/v) (λ_{ex} = 396 nm, slit: 10 nm/10 nm). Inset: visual fluorescence changes of probe upon addition of Zn^{2+} under illumination with a 365 nm UV lamp.

Fig. 4. Optical density two-dimensional graph of the probe at 504 nm, respectively upon the addition of several metal ions (including Li^+, K^+, Ca^{2+}, Na^+, Mg^{2+}, Al^{3+}, Ba^{2+}, Fe^{3+}, Co^{2+}, Ni^{2+}, Cu^{2+}, Mn^{2+}, Cr^{2+}, Cd^{2+}, Pb^{2+}, Ag^+). Inset: a color change photograph for Zn^{2+} and the other metal ions under illumination with a 365 nm UV lamp.
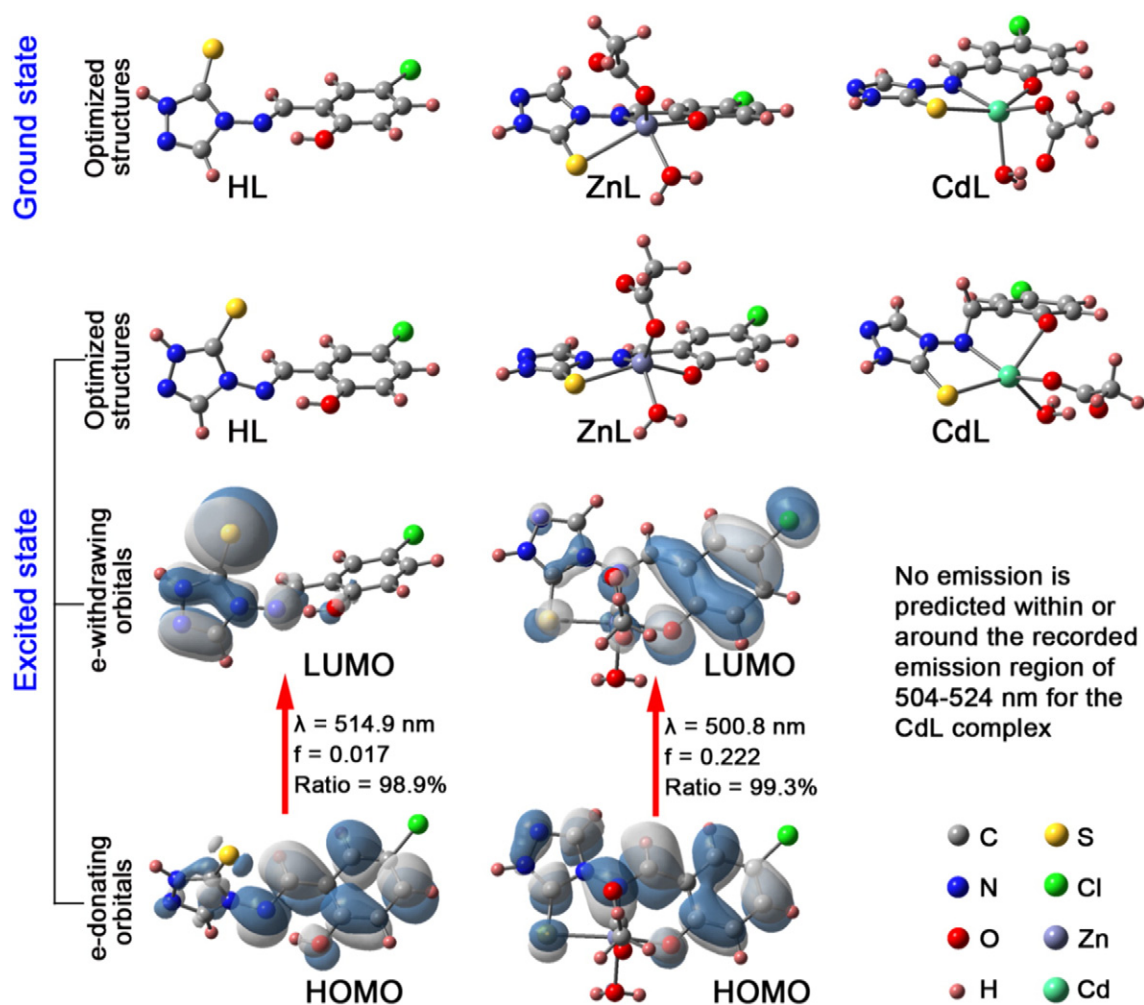
Fig. 5. The ground and excited states optimized structures of L, ZnL, and CdL and the emission mechanism for HL and ZnL predicted by the TD-DFT calculations. "f" near the red arrow denotes the oscillator strengths of the emission.

are not coplanar (the dihedral angles (δ) are 45.5° and 38.0°, respectively) in the ground state optimized structures of the free HL probe and the complex ZnL, while that in the complex CdL is almost coplanar ($\delta = 7.1°$). In contrast, the dihedral angle (δ) in the excited state optimizations displays significantly different changes. The δ value for HL becomes wider ($\delta = 75.7°$), the two rings of the Schiff base in ZnL is almost planar ($\delta = 4.6°$), while that in CdL becomes non-coplanar ($\delta = 35.2°$) and the structure is distorted severely. The results indicated that the fluorescence of HL should be weak but that of ZnL will be very intense. Because the rigid coplanar structure in ZnL can reduce the non-radiative transition probabilities and significantly improve the radiative transition probabilities, resulting in a large fluorescence enhancement. This indicates that the probe HL is a typical chelation-enhanced fluorescence (CHEF)-type sensor. The 1,2,4-triazole ring and benzene ring of the Schiff base parts in CdL becomes non-coplanar, together with the severely distorted structure (relative to the its ground state structure with almost planar L ligand), which may result in the very week fluorescence of CdL.

As shown in Fig. 5, the predicted emission for HL and ZnL are at 514.9 and 500.8 nm, which are very close to the experimental recorded 524 and 504 nm, respectively. The predicted emission wavelength also show a blue shift (from 514.9 to 500.8 nm) when the Zn-complex is formed. The oscillator strengths (f) for HL and ZnL are 0.017 and 0.222, respectively, which are consistent with the fact that the emission of ZnL is much more intense than that of HL. Note that emission peaks of CdL are much different from those of HL and ZnL and the most important

difference is that there is no peak around the experimental recorded peak(s) (the nearest peaks are at 573.9 and 395.0 nm, respectively), which is consistent with above discussion. We speculate that the slight emission around 510 in experimental fluorescence may be generated by the free HL probe. These calculation results show the excellent agreement with experiments, which makes it reasonable to discuss the emission mechanism based on theoretical calculations.

According to the calculation results, the emission of free HL probe and ZnL both originated from the transition of the electrons in their HOMO (π orbital) to LUMO (π orbital), showing the obvious $\pi^* \rightarrow \pi$ characters. The ratios of 98.9% and 99.3% suggest the rather simple transition manner. However, why are emission intensities of HL and ZnL so different? The answer can be found from the differences in their excited state equilibrium geometries and the MOs related to the transition. As Fig. 5 shows, the e-donating HOMO of HL is a π orbital distributed mainly on the benzene ring of the Schiff base and the e-accepting LUMO is also a π orbital but distributed mainly on 1,2,4-triazole ring. Since there is a dihedral angle of 75.7° in the two parts, it will be hard to transit the π electrons from the benzene ring of the Schiff base to the 1,2,4-triazole ring, which results in the weak emission of HL and the small oscillator strength (0.017). In contrast, the e-donating HOMO of ZnL is a π orbital distributed on whole ligand and the e-accepting LUMO is a π orbital distributed mainly on the benzene ring of the Schiff base. As the ligand is almost planar, it should be very easy to transit the π electrons from the HOMO to LUMO. Such a conclusion can be demonstrated by the intense emission of ZnL and the large oscillator strength (0.222).

4. Conclusion

In conclusion, we have shown that the fluorescent probe 4-(5-Chloro-2-hydroxylbenzylideneamino)-1H-1,2,4-triazole-5(4H)-thione (HL) senses Zn^{2+} ion with high sensitivity and selectivity in aqueous medium (DMSO/H_2O, 1:9, v/v). The probe HL binding with 1:1 stoichiometry to Zn^{2+} is confirmed by Uv–Vis titration experiment and job's plot study. Furthermore, the photo-physical properties of ZnL are demonstrated and the detection mechanism of this sensor for Zn ion is evaluated by computer theoretical calculation. The results indicate that the coordination of zinc ion to HL enhance the rigidity of the ligand, thus greatly reducing the non-radiative transition probabilities, resulting in the fluorescence intensity of the complex ZnL increased. The Schiff base probe may act as a good candidate for detection Zn^{2+} ion due to its high selectivity over other common metals, even Cd^{2+}, and the detection limit as low as 51 nmol/L.

Acknowledgments

Appendix A. Supplementary data

Supplementary data to this article can be found online at http://dx.doi.org/10.1016/j.saa.2015.10.035.

References

[1] S. Frassinetti, G. Bronzetti, L. Caltavuturo, M. Cini, C.D. Croce, J. Environ. Pathol. Toxicol. Oncol. 25 (2006) 597–610.
[2] J. Osredkar, N. Sustar, J Clinic. Toxicol. S3 (2011) 001, http://dx.doi.org/10.4172/2161-0495.
[3] J. Berg, Y. Shi, Science 271 (1996) 1081–1085.
[4] K.H. Falchuk, Mol. Cell. Biochem. 188 (1998) 41–48.
[5] E. Tomat, S.J. Lippard, Curr. Opin. Chem. Biol. 14 (2010) 225–230.
[6] C.R.T. Tarley, F.N. Andrade, F.M. de Oliveira, M.Z. Corazza, L.F.M. de Azevedo, M.G. Segatelli, Anal. Chim. Acta 703 (2011) 145–151.
[7] L. Zhao, S. Zhong, K. Fang, Z. Qian, J. Chen, Hazard. Mater. 239–240 (2012) 206–212.
[8] H. Karami, M.F. Mousavi, Y. Yamini, M. Shamsipur, Anal. Chim. Acta 509 (2004) 89–94.
[9] F. Tormaa, M. Kadar, K. Toth, E. Tatar, Nafion, Anal. Chim. Acta 619 (2008) 173–182.
[10] H.-M. Liu, P. Venkatesan, S.-P. Wu, Sensors Actuators B Chem. 203 (2014) 719–725.
[11] E.M. Nolan, S.J. Lippard, Acc. Chem. Res. 42 (2009) 193–203.
[12] A.N. Gusev, S. Shulgin, S. Meshkova, S. Smola, W. Linert, J. Lumin. 155 (2014) 311–316.
[13] Z.C. Xu, J. Yoon, D.R. Spring, Chem. Soc. Rev. 39 (2010) 1996–2006.
[14] X. Li, X. Gao, W. Shi, H. Ma, Chem. Rev. 114 (2014) 590–659.
[15] K.P. Carter, A.M. Young, A.E. Palmer, Chem. Rev. 114 (2014) 4564–4601.
[16] E. Kimura, T. Koike, Chem. Soc. Rev. 27 (1998) 179–184.
[17] V.K. Gupta, N. Mergu, A.K. Singh, Sensors Actuators B Chem. 202 (2014) 674–682.
[18] M. Zhang, W. Lu, J. Zhou, G. Du, L. Jiang, J. Ling, Z. Shen, Tetrahedron 70 (2014) 1011–1015.
[19] A. Avci, I. Kaya, Tetrahedron Lett. 56 (2015) 1820–1824.
[20] H. Kim, G.R. You, G.J. Park, J.Y. Choi, I. Noh, Y. Kim, S.J. Kim, C. Kim, R.G. Harrison, Dyes Pigments 113 (2015) 723–729.
[21] S. Jana, S. Dalapati, M.A. Alam, N. Guchhait, J. Photochem. Photobiol. A Chem. 238 (2012) 7–15.
[22] J.R. Lin, C.J. Chu, P. Venkatesan, S.P. Wu, Sensors Actuators B Chem. 207 (2015) 563–570.
[23] W. Chyan, D.Y. Zhang, S.J. Lippard, R.J. Radford, Proc. Natl. Acad. Sci. 111 (2014) 143–148.
[24] P.W. Du, S.J. Lippard, Inorg. Chem. 49 (2010) 10753–10755.
[25] L.J. Tang, X. Dai, K.L. Zhong, D. Wu, X. Wen, Sensors Actuators B Chem. 203 (2014) 557–564.
[26] H.L. Chen, Y.B. Wu, Y.F. Cheng, H. Yang, F.Y. Li, P. Yang, C.H. Huang, Inorg. Chem. Commun. 10 (2007) 1413–1415.
[27] L.J. Qu, C.X. Yin, F.J. Huo, J.B. Chao, Y.B. Zhang, F.Q. Cheng, Sensors Actuators B Chem. 191 (2014) 158–164.
[28] K.B. Kim, H. Kim, E.J. Song, S. Kim, I. Noh, C. Kim, Dalton Trans. 42 (2013) 16569–16577.
[29] T. Xu, H.D. Duan, X.J. Wang, X. Meng, J. Bu, Spectrochim. Acta A 138 (2015) 603–608.
[30] S.B. Liu, C.F. Bi, Y.H. Fan, Y. Zhao, P.F. Zhang, Q.D. Luo, D.M. Zhang, Inorg. Chem. Commun. 14 (2011) 1297–1301.
[31] M. Hosseini, A. Ghafarloo, M.R. Ganjali, F. Faridbod, P. Norouzi, M.S. Niasari, Sensors Actuators B Chem. 198 (2014) 411–415.
[32] S. Sinha, T. Mukherjee, J. Mathew, S.K. Mukhopadhyay, S. Ghosh, Anal. Chim. Acta 822 (2014) 60–68.
[33] W.H. Hsieh, C.F. Wan, D.J. Liao, A.T. Wu, Tetrahedron Lett. 53 (2012) 5848–5851.
[34] M.H. Yan, T.R. Li, Z.Y. Yang, Inorg. Chem. Commun. 14 (2011) 463–465.
[35] S. Chall, S.S. Mati, S. Konar, D. Singharoy, S.C. Bhattacharya, Org. Biomol. Chem. 12 (2014) 6447–6456.
[36] A. Ganguly, B.K. Paul, S. Ghosh, S. Kar, N. Guchhait, Analyst 138 (2013) 6532–6541.
[37] A.X. Ding, F. Tang, T. Wang, X.T. Tao, J.X. Yang, J. Chem. Sci. 127 (2015) 375–382.
[38] N. Roy, H.A.R. Pramanik, P.C. Paul, T.S. Singh, Spectrochim. Acta A 140 (2015) 150–155.
[39] Z. Dong, X. Le, P. Zhou, C. Dong, J. Ma, RSC Adv. 4 (2014) 18270–18277.
[40] M. Hosseini, Z. Vaezi, M.R. Ganjali, F. Faridbod, S.D. Abkenar, K. Alizadeh, M. Salavati-Niasari, Spectrochim. Acta A 75 (2010) 978–982.
[41] K. Tayade, S.K. Sahoo, B. Bondhopadhyay, V.K. Bhardwaj, N. Singh, A. Basu, R. Bendre, A. Kuwar, Biosens. Bioelectron. 61 (2014) 429–433.
[42] K. Tayade, S.K. Sahoo, R. Patil, N. Singh, S. Attarde, A. Kuwar, Spectrochim. Acta A 126 (2014) 312–316.
[43] U.A. Fegade, S.K. Sahoo, A. Singh, N. Singh, S.B. Attarde, A.S. Kuwar, Anal. Chim. Acta 872 (2015) 63–69.
[44] N. Khairnar, K. Tayade, S.K. Sahoo, B. Bondhopahyay, A. Bacu, J. Singh, N. Singh, V. Gite, A. Kuwar, Dalton Trans. 44 (2015) 2097–2102.
[45] M. Iniya, D. Jeyanthi, K. Krishnaveni, A. Mahesh, D. Chellapp, Spectrochim. Acta A 120 (2014) 40–46.
[46] S.Y. Park, J.H. Yoon, C.S. Hong, R. Souane, J.S. Kim, S.E. Matthews, J. Organomet. Chem. 73 (2008) 8212–8218.
[47] E. Hao, T. Meng, M. Zhang, W. Pang, Y. Zhou, L. Jiao, J. Phys. Chem. A 115 (2011) 8234–8241.
[48] S.A. Ingale, F. Seela, J. Organomet. Chem. 77 (2012) 9352–9356.
[49] J. Zhou, W. Lu, F. Hu, M. Zhang, L. Jiang, Z. Shen, J. Polym. Sci., Polym. Chem. Ed. 52 (2014) 2248–2257.
[50] J.R. Reid, N.D. Heindel, J. Heterocycl. Chem. 13 (1976) 925–926.
[51] C.X. Yuan, X.M. Yao, M.L. Zhu, H.M. Zhu, Acta Crystallogr. E70 (2014) o574–o575.
[52] S. Shit, J. Chakraborty, B. Samanta, G.M. Rosair, S. Mitra, Z. Naturforsch. 64b (2009) 403–408.
[53] T.B.S.A. Ravoof, S.A. Omar, M.I. Mohamed Tahir, K.A. Crouse, Acta Crystallogr. E68 (2012) M534–m535.
[54] O.P. Anderson, A. la Cour, M. Findeisen, L. Hennig, O. Simonsen, L.F. Taylor, H. Toftlund, J. Chem. Soc. Dalton Trans. 111–120 (1997).